

Simple inhibitors of histone deacetylase activity that combine features of short-chain fatty acid and hydroxamic acid inhibitors

JESSICA L. TISCHLER¹, BASEL ABUAITA¹, SIERRA C. CUTHPERT¹, CHRISTOPHER FAGE¹, KRISTI MURPHY¹, ANDREW SAXE², EDWARD B. FURR³, JAMIE HEDRICK³, JENNIFER MEYERS³, DAVID SNARE³, & ALI R. ZAND³

¹Department of Chemistry and Biochemistry, University of Michigan-Flint, Flint, MI, USA, ²McLaren Regional Medical Center, Flint, MI, USA, and ³Department of Science and Mathematics, Kettering University, Flint, MI, USA

(Received 24 April 2007; in final form 4 September 2007)

Abstract

Butyric acid and trichostatin A (TSA) are anti-cancer compounds that cause the upregulation of genes involved in differentiation and cell cycle regulation by inhibiting histone deacetylase (HDAC) activity. In this study we have synthesized and evaluated compounds that combine the bioavailability of short-chain fatty acids, like butyric acid, with the bidentate binding ability of TSA. A series of analogs were made to examine the effects of chain length, simple aromatic cap groups, and substituted hydroxamates on the compounds' ability to inhibit rat-liver HDAC using a fluorometric assay. In keeping with previous structure-activity relationships, the most effective inhibitors consisted of longer chains and hydroxamic acid groups. It was found that 5-phenylvaleric hydroxamic acid and 4-benzoylbutyric hydroxamic acid were the most potent inhibitors with IC₅₀'s of 5 μM and 133 μM respectively.

Keywords: *Histone deacetylase, short-chain fatty acid, hydroxamic acid, inhibitor, cancer*

Introduction

Reversible modification of chromatin's structure plays a fundamental role in regulating gene transcription. Histone acetyltransferases (HATs) and histone deacetylases (HDACs) are enzymes that work in tandem to acetylate and deacetylate the ε-amino groups on the lysine residues located in the N-terminal region of the core histone proteins [1–3]. Acetylation of these residues by HATs neutralizes the histones' positive charge and decreases the DNA's affinity for the protein. The DNA then unwinds and allows the cell's transcriptional machinery access to the strand thereby promoting gene expression. HDACs reverse this process by cleaving the acetyl groups. This results in a closed chromatin structure and the repression of gene expression. Inhibition of HDAC activity

therefore has the effect of promoting the transcription of silenced genes. Application of HDAC inhibitors in cancer cell lines and mouse model systems leads to interruption of the cell cycle, differentiation, and apoptosis [3–6]. Clinical studies have shown tumor repression and improvement of patient symptoms without significant side effects. These therapeutic effects are a result of increased expression of proteins such as p21^{WAF1/CIP1}, FAS, and caspase 3 [7–9].

Structure-activity relationship studies of various HDAC enzymes and X-ray crystal structures of inhibitors bound to a histone deacetylase-like protein (HDLP) from *Aquifex aeolicus* have elucidated HDACs' conserved active site [10–12]. Hydrolysis of the acetylated lysine residue is promoted by coordination of the carbonyl oxygen with a Zn⁺²

Correspondence: J.L. Tischler, Department of Chemistry and Biochemistry, University of Michigan-Flint, 303 E. Kearsley St., Flint, MI 48502, USA. Fax: 810-766-6693. E-mail: jtisch@umflint.edu. A.R. Zand, Department of Science and Mathematics, Kettering University, 1700 W. Third Ave., Flint, MI 48504, USA. Fax: 810-762-7979. E-mail: azand@kettering.edu

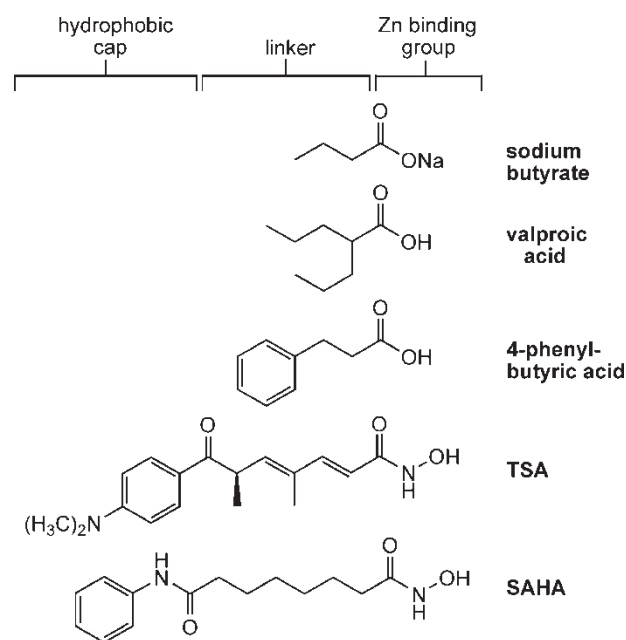


Figure 1. Structures of known HDAC inhibitors.

cation. The Zn^{+2} cation lies at the bottom of a hydrophobic channel, greatly influencing the structure of inhibitors. Although many classes of inhibitors have been developed, they all have a Zn-binding moiety located at the end of hydrophobic linker chain for proper placement in this channel (Figure 1). Opposite the Zn-binding group, most inhibitors incorporate a hydrophobic cap structure that has been shown to interact with aromatic residues at the mouth of the channel. Consequently, many of these groups are aromatic in nature, but can vary greatly in size and secondary functionality.

One of the first compounds found to inhibit HDAC was sodium butyrate (Figure 1). It is representative of the short-chain fatty acid class of inhibitors. A fatty acid found naturally in the body, its biological effects have been well studied [13,14]. Although a non-specific, millimolar level inhibitor of HDAC, it has been found to induce differentiation in neuroblastoma cells, human ovarian carcinoma cells, and leukemia cells, among others [13]. However, rapid metabolism has limited its clinical development due to the need for constant infusion to maintain bioactive levels [15]. Investigations of other short chain acids, such as 4-phenylbutyric acid and valproic acid (Figure 1), have shown them to be effective against similar cancer cell lines [16,17]. Although 4-phenylbutyric acid's *in vitro* efficacy is low, it was the first HDAC inhibitor to be evaluated in clinical trials [3]. Valproic acid, a drug currently used to treat epilepsy and bipolar disorder, has a significantly longer half-life than sodium butyrate and has an established clinical record [16]. Depending on the type of HDAC studied, IC_{50} values for valproic acid have been measured between

0.5 – 2 mM [18,19]. Despite its low potency, valproic acid was studied as a combination therapy with retinoic acid in patients with acute myeloid leukemia [20].

Originally isolated from *Streptomyces hygroscopicus* as an antifungal antibiotic agent, (*R*)-Trichostatin A (TSA) (Figure 1) was found to induce cell differentiation [4,21]. Further studies revealed HDACs to be its molecular target. TSA, with its ability to bind Zn^{+2} in a bidentate fashion, not only is one of the most potent inhibitors of HDAC with an IC_{50} less than 10 nM, but it also spawned the investigation into the largest class of HDAC inhibitors — the hydroxamic acids. Studies with hydroxamic acids and longer chain fatty acids led to the development of suberoylanilide hydroxamic acid (SAHA) (Figure 1), which is currently in phase III clinical trials [3,22]. Crystallographic studies of TSA and SAHA bound to HDLP show that the hydroxamic acid not only provides additional binding to the Zn^{+2} via the N-hydroxyl group, but the nitrogen and hydroxyl species also serve as H-bond donors to active-site histidines. Although SAHA is expected to be introduced on the market in the near future [23], TSA has had limited clinical success. TSA is now commercially available in enantiopure form, but the costly asymmetric synthesis hampers its pharmaceutical development. An earlier study with mouse xenographs also showed no antitumor activity. It was suggested that this could be due in part to TSA's poor solubility [24]. There is also mixed data regarding the toxicity of hydroxamic acids in general. Multiple animal and clinical studies on TSA and SAHA have not shown general toxicity or teratogenicity [25]. However, earlier studies of hydroxamic acid metabolism show that hydrolysis can produce hydroxylamine, which is a potential mutagen [26]. Pharmacokinetic studies of TSA have shown that hydroxamic acids are prone to glucuronidation, sulfonation, and reduction to the amide [26]. Enolization to the *S*-enantiomer or hydrolysis to the corresponding carboxylic acid also results in inactivity. This metabolic instability results in a relatively short half-life *in vivo* [28].

The goals of this study are to combine the beneficial structural features of both short-chain fatty acids and hydroxamic acids. Short-chain acids have improved solubility, low toxicity, and are relatively easy to obtain and derivitize. Hydroxamates provide increased inhibition via bidentate binding to the Zn^{+2} and additional hydrogen bonds. 5-Phenylvaleric acid, 3-benzoylpropanoic acid, 3-benzoylbenzoic acid, and 4-benzoylbenzoic acid were selected as synthetic starting points not only for their similarity to 4-phenylbutyric acid, but because they are relatively inexpensive and commercially available. 4-Phenylbutyric acid derivatives were also developed for comparison. The hydroxamic acid, N-methyl hydroxamate and N,O-dimethyl hydroxamate derivatives of

these compounds were synthesized and their inhibition of rat-liver HDAC was investigated. The methylated hydroxamates were developed as potential alternatives to hydroxamic acids. It is hypothesized that these compounds will still bind to the Zn^{+2} in a bidentate fashion while potentially reducing the metabolic concerns. Because the methyl groups could lead to negative steric interactions and eliminate key hydrogen bonds, the inhibition of these compounds was compared to the corresponding carboxylic and hydroxamic acids in this study.

Materials and methods

General

All of the carboxylic acid starting materials were purchased from Aldrich (Milwaukee, WI) and were used without further purification. 1H and ^{13}C NMR spectra were obtained using a 300 MHz Varian Gemini instrument. FTIR spectra were obtained using either a Thermo Nicolet Avatar 360 FT-IR ESP or a MIDAC M series FTIR. Elemental analysis was performed using a Perkin-Elmer 2400 series II CHN analyzer. Mass spectroscopy data was obtained using a Micromass LCT Time-of-Flight Mass Spectrometer with Electrospray and APCI. Elemental analysis and mass spectroscopy studies were performed by the Department of Chemistry's facilities at the University of Michigan in Ann Arbor, MI.

General procedure for synthesis of hydroxamates

The desired carboxylic acid (0.1 moles) was added to 150 mL of dry THF in a nitrogen flushed flask. N-methylmorpholine (0.1 moles) was added and the solution/mixture was stirred at room temperature under nitrogen atmosphere for 0.5 h. Isopropyl chloroformate (0.12 moles) was added drop-wise producing a cloudy solution. This mixture was stirred at room temperature for 2.5 h before a solution containing the desired hydroxylamine (0.12 moles) and N-methylmorpholine (0.12 moles) in dry acetonitrile was added. The resulting mixture was stirred overnight. Following removal of the solvent using rotary evaporation, the resulting slurry was dissolved in 10% HCl and extracted three times with ethyl acetate. The combined organic layers were extracted twice with saturated sodium carbonate, followed by sodium chloride, and then dried over anhydrous magnesium sulfate. The solvent was evaporated to yield a yellowish oil which was chromatographed, using hexane/ethyl acetate mixtures (gradient chromatography) as eluent, to yield white or off-white solids or oils as products (Figure 2). Yields ranged from 68% to 80%.

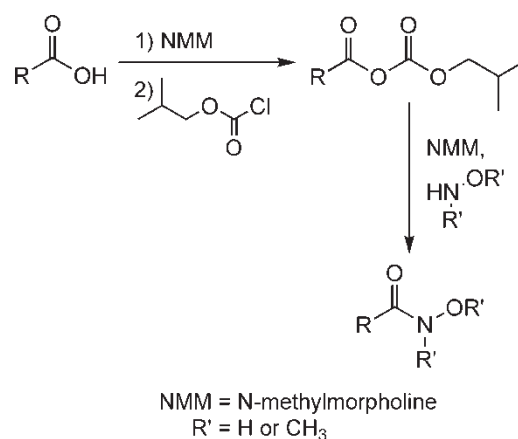


Figure 2. General synthesis of hydroxamate, N-methylhydroxamates, and N,O-dimethylhydroxamates.

4-Phenylbutyric acid hydroxamate (2). Melting point: 73–77°C. 1H NMR ($CDCl_3$): δ 1.95 (quintet, $J = 7.5$ Hz, 2H), 2.36 (t, $J = 7.5$ Hz, 2H), 2.66 (t, $J = 7.8$ Hz, 2H), 7.18 (distorted triplet, $J = 8.1$ Hz, 3H), 7.27 (distorted triplet, $J = 7.8$ Hz, 2H), 9.6 (broad singlet). ^{13}C NMR ($CDCl_3$): δ 30.4, 32.34, 35.20, 125.5, 128.01, 128.09, 141.7, 171.5. IR (KBr) cm^{-1} : 3241, 3055, 3029, 2962, 1787, 1710, 1454, 1266, 1107. EA: Found: 66.92% C, 7.31% H, 7.81% N. Calculated: 67.02%, 7.31% H, 7.82% N.

4-Phenylbutyric acid N-methylhydroxamate (3). 1H NMR ($CDCl_3$): δ 2.0 (quintet, $J = 7.2$ Hz, 2H), 2.42 (t, $J = 7.5$ Hz, 2H), 2.68 (t, $J = 7.8$ Hz, 2H), 3.14 (singlet, 3H), 7.15 (distorted triplet, $J = 8.1$ Hz, 3H), 7.29 (distorted triplet, $J = 7.8$ Hz, 2H), 9.5 (broad Singlet). ^{13}C NMR ($CDCl_3$): δ 30.84, 31.6, 35.42, 35.77, 125.44, 128.04, 128.1, 141.9, 174.7. IR (neat) cm^{-1} : 3175, 3031, 2939, 2864, 1618, 1490, 1201. EA: Found: 67.90% C, 7.92% H, 6.71% N. Calculated: 68.37% C, 7.32% H, 7.25% N.

4-Phenylbutyric acid N,O-dimethylhydroxamate (4). 1H NMR ($CDCl_3$): δ 1.97 (quintet, $J = 7.5$ Hz, 2H), 2.38 (t, $J = 7.5$ Hz, 2H), 2.63 (t, $J = 7.8$ Hz, 2H), 3.1 (singlet, 3H), 3.6 (singlet, 3H), 7.17 (distorted triplet, $J = 8.1$ Hz, 3H), 7.27 (distorted triplet, $J = 7.8$ Hz, 2H). ^{13}C NMR ($CDCl_3$): δ 30.85, 32.26, 35.34, 35.86, 60.52, 125.48, 128.04, 128.1, 141.7, 174.6. IR (neat) cm^{-1} : 2938, 2868, 1672, 1497, 1387, 1094. MS: $[M + Na]^+ = 230.1151$. Calculated: 230.1157.

5-Phenylvaleric acid hydroxamate (6). Melting point: 49–53°C. 1H NMR ($CDCl_3$): δ 1.66 (quintet, $J = 3$ Hz, 4H), 2.48 (t, $J = 6$ Hz, 2H), 2.59 (t, $J = 3$ Hz, 2H), 4.2 (broad), 7.2 (distorted triplet,

$J = 6.6$ Hz, 3H), 7.31 (distorted triplet, $J = 6.6$ Hz, 2H), 9.5 (broad singlet). ^{13}C NMR (CDCl_3): δ 24.72, 30.41, 32.3, 35.15, 125.48, 128.0, 128.1, 141.72, 171.4. IR (KBr) cm^{-1} : 3202, 3030, 2928, 2861, 1618, 1458. MS: $[\text{M} + \text{H}]^+ = 294.1172$. Calculated: 294.1172.

5-Phenylvaleric acid N-methylhydroxamate (7). ^1H NMR (CDCl_3): δ 1.70 (quintet, $J = 3$ Hz, 4H), 2.58 (t, $J = 6$ Hz, 2H), 2.66 (t, $J = 3$ Hz, 2H), 3.26 (s, 3H), 7.2 (distorted triplet, $J = 6.6$ Hz, 3H), 7.29 (distorted triplet, $J = 6.6$ Hz, 2H), 9.5 (broad singlet). ^{13}C NMR (CDCl_3): δ 24.28, 30.94, 31.76, 35.4, 35.8, 125.48, 128.04, 128.1, 141.95, 174.4. IR (neat) cm^{-1} : 3190, 3023, 2939, 2871, 1611, 1497, 1459, 1383, 1201. MS: $[\text{M} + \text{H}]^+ = 208.1336$. Calculated: 208.1338.

5-Phenylvaleric acid N,O-dimethylhydroxamate (8). ^1H NMR (CDCl_3): δ 1.72 (quintet, $J = 3$ Hz, 4H), 2.50 (t, $J = 6$ Hz, 2H), 2.62 (t, $J = 3$ Hz, 2H), 3.16 (s, 3H), 3.72 (s, 3H), 7.2 (distorted triplet, $J = 6.6$ Hz, 3H), 7.29 (distorted triplet, $J = 6.6$ Hz, 2H). ^{13}C NMR (CDCl_3): δ 24.30, 30.85, 32.26, 35.34, 35.86, 60.52, 125.48, 128.04, 128.1, 141.95, 174.6. IR (neat) cm^{-1} : 3084, 3031, 2939, 2864, 1672, 1452, 1383. EA: Found: 70.55% C, 8.59% H, 5.91% N. Calculated: 70.56% C, 8.65% H, 6.33% N.

3-Benzoylpropanoic acid hydroxamate (10). Melting point: 96–98°C. ^1H NMR (CDCl_3): δ 2.92 (t, $J = 6.6$ Hz, 2H), 3.37 (t, $J = 6.6$ Hz, 2H), 7.45 (tt, $J = 7.2$ Hz, $J = 1.2$ Hz, 2H), 7.53 (tt, $J = 7.5$ Hz, $J = 1.2$ Hz, 1H), 8.0 (dt, $J = 6.9$ Hz, $J = 1.8$ Hz, 2H), 9.6 (broad singlet, 1H). ^{13}C NMR (CDCl_3): δ 25.6, 31.4, 127.7, 128.33, 132.7, 136.3, 172.9, 198.3. IR (KBr) cm^{-1} : 3405, 3055, 2987, 1686, 1627, 1449, 1422, 1267. EA: Found: 62.14% C, 5.76% H, 7.24% N. Calculated: 62.17% C, 5.74% H, 7.25% N.

3-Benzoylpropanoic acid N-methylhydroxamate (11). Melting point: 103–105°C. ^1H NMR (CDCl_3): δ 2.85 (t, $J = 6.6$ Hz, 2H), 3.2 (s, 3H), 3.28 (t, $J = 6.6$ Hz, 2H), 7.43 (tt, $J = 7.2$ Hz, $J = 1.2$ Hz, 2H), 7.6 (tt, $J = 7.5$ Hz, $J = 1.2$ Hz, 1H), 8.02 (dt, $J = 6.9$ Hz, $J = 1.8$ Hz, 2H), 9.44 (broad singlet, 1H). ^{13}C NMR (CDCl_3): δ 25.56, 31.8, 32.52, 127.59, 128.3, 132.66, 136.3, 172.8, 198.7. IR (KBr) cm^{-1} : 3144, 2944, 2876, 2718, 1674, 1603, 1508, 1201. EA: Found: 63.65% C, 6.56% H, 6.83% N. Calculated: 63.76% C, 6.32% H, 6.76% N.

3-Benzoylpropanoic acid N,O-dimethylhydroxamate (12). ^1H NMR (CDCl_3): δ 2.87 (t, $J = 6.6$ Hz, 2H), 3.18 (s, 3H), 3.32 (t, $J = 6.6$ Hz, 2H), 3.753 (s, 3H), 7.43 (tt, $J = 7.2$ Hz, $J = 1.2$ Hz, 2H), 7.53 (tt, $J = 7.5$ Hz, $J = 1.2$ Hz, 1H), 7.98 (dt, $J = 6.9$ Hz, $J = 1.8$ Hz, 2H). ^{13}C NMR (CDCl_3): δ 25.62, 31.78, 32.52, 60.79, 127.63, 128.13, 132.73, 136.33, 172.85, 198.49. IR (neat) cm^{-1} : 3065, 2669, 2940, 2917, 1682, 1661, 1449, 1362, 1242, 1181, 1001. EA: Found: 65.24% C, 6.96% H, 5.39% N. Calculated: 65.14% C, 6.83% H, 6.33% N.

3-Benzoylbenzoic acid hydroxamate (14). Melting point: 147–148°C. ^1H NMR (CDCl_3): δ 7.35 (m, 3H), 7.49 (t, $J = 7.5$ Hz), 7.69 (m, 4H), 7.94 (broad singlet, 1H), 9.50 (broad, 1H). ^{13}C NMR (CDCl_3): δ 128.2, 129.4, 129.82, 131.62, 132.38, 136.45, 137.7, 171.4, 196.1. IR (KBr) cm^{-1} : 3318, 3059, 2816, 1653, 1622, 1561, 1285. EA: Found: 69.90% C, 4.79% H, 5.87% N. Calculated: 69.70% C, 4.60% H, 5.81% N.

3-Benzoylbenzoic acid N-methylhydroxamate (15). Melting point: 81–83°C. ^1H NMR (CDCl_3): δ 3.25 (s, 3H), 7.40 (m, 3H), 7.53 (t, $J = 7.5$ Hz), 7.72 (m, 4H), 7.9 (broad singlet, 1H), 9.34 (broad, 1H, OH). ^{13}C NMR (CDCl_3): δ 36.9, 128.3, 129.32, 129.76, 131.72, 132.6, 136.4, 137.7, 172.1, 195.5. IR (KBr) cm^{-1} : 3117, 3059, 2816, 1667, 1613, 1578, 1323, 1275, 1215. EA: Found: 70.56% C, 5.47% H, 5.42% N. Calculated: 70.58% C, 5.13% H, 5.49% N.

3-Benzoylbenzoic acid N,O-dimethylhydroxamate (16). ^1H NMR (CDCl_3): δ 3.25 (s, 3H), 3.77 (s, 3H), 7.37 (m, 3H), 7.50 (t, $J = 7.5$ Hz), 7.67 (m, 4H), 7.90 (broad singlet, 1H). ^{13}C NMR (CDCl_3): δ 37.8, 61.14, 128.12, 129.27, 129.7, 131.66, 132.58, 136.42, 137.7, 171.09, 195.8, 171.09, 195.8. IR (neat) cm^{-1} : 3067, 2938, 1780, 1723, 1661, 1447, 1279, 1172. MS: $[\text{M} + \text{Na}]^+ = 292.0948$. Calculated: 292.0950.

4-Benzoylbutyric acid hydroxamate (18). Melting point: 115–118°C. ^1H NMR (CDCl_3): δ 2.0 (quintet, $J = 6.9$ Hz, 2H), 2.42 (broad triplet, $J = 6.9$ Hz, 2H), 2.97 (t, $J = 7.2$ Hz, 2H), 7.37 (t, $J = 7.2$ Hz, 2H), 7.47 (t, $J = 7.5$ Hz, 1H), 7.90 (d, $J = 7.5$ Hz, 2H). ^{13}C NMR (CDCl_3): δ 18.65, 30.42, 31.58, 127.8, 128.2, 132.63, 136.50, 173.62, 199.7. IR (KBr) cm^{-1} : 3177, 3065, 3027, 2926, 1744, 1707, 1611, 1453. EA: Measured: 63.42% C, 6.43% H, 9.19% N. Calculated: 63.76% C, 6.32% H, 6.76% N.

4-Benzoylbutyric acid N-methylhydroxamate (19). Melting point: 89–91°C. ^1H NMR (CDCl_3): δ 2.08 (quintet, $J = 6.9$ Hz, 2H), 2.45 (broad triplet, $J = 6.9$ Hz, 2H), 3.05 (t, $J = 7.2$ Hz, 2H), 3.17 (s, 3H), 7.37 (t, $J = 7.2$ Hz, 2H), 7.47 (t, $J = 7.5$ Hz, 1H), 7.90 (d, $J = 7.5$ Hz, 2H). ^{13}C NMR (CDCl_3): δ 18.42, 30.60, 31.6, 37.2, 127.7, 128.31, 132.46, 136.7, 173.5, 199.2. IR (KBr) cm^{-1} : 3175, 2897, 1672, 1611, 1447, 1181. EA: Found: 65.30% C, 7.19% H, 6.22% N. Calculated: 65.14% C, 6.83% H, 6.33% N.

4-Benzoylbutyric acid N,O-dimethylhydroxamate (20). ^1H NMR (CDCl_3): δ 2.01 (quintet, $J = 6.9$ Hz, 2H), 2.48 (broad triplet, $J = 6.9$ Hz, 2H), 3.01 (t, $J = 7.2$ Hz, 2H), 3.10 (s, 3H), 3.59 (s, 3H), 7.37 (t, $J = 7.2$ Hz, 2H), 7.47 (t, $J = 7.5$ Hz, 1H), 7.90 (d, $J = 7.5$ Hz, 2H). ^{13}C NMR (CDCl_3): δ 18.71, 30.52, 31.78, 37.35, 60.8, 127.7, 128.2, 132.6, 136.47, 173.7, 199.5. IR (neat) cm^{-1} : 3061, 2940, 1686, 1449, 1231, 1185, 993. MS: $[\text{M} + \text{Na}]^+ = 258.1112$. Calculated: 258.1106.

HDAC assay

Assay of HDAC activity was modified from the method of Wegener [29]. The assay is a two-step reaction. During the first step, HDAC deacetylates the ϵ -acetylated lysine residue of the substrate. In the second step, 4-amino-7-methylcoumarin is cleaved from the deacetylated substrate using trypsin, causing a significant increase in fluorescence compared to the acetylated substrate. Assays were run in triplicate with positive and negative controls in at least three separate experiments.

The peptide substrate of AC-Arg-Gly-Lys(AC)-AMC (Bachem, USA; 5 mg) was initially dissolved in DMSO and diluted in HDAC buffer (15 mM Tris-HCl [pH 8.1], 250 μM EDTA, 250 mM NaCl, 10% glycerol) to give a 1 mM solution. Rat liver HDAC (Calbiochem, Germany; 89 U/mL) was diluted in HDAC buffer. Stock solutions of all inhibitors were made in DMSO.

Enzyme reactions were prepared by combining HDAC buffer, the diluted enzyme (3 U/mL), and 10 μL of inhibitor stock solutions to achieve a final concentration of 10% DMSO. Following 5 min of incubation at 30°C, the reaction was initiated by the addition of substrate (300 μM) to bring the total volume to 100 μL . Following a second incubation at 30°C for 1 h, 100 μL of stop solution was added (10 mg/mL trypsin in 50 mM Tris-HCl [pH 8.0], 100 mM NaCl, 2 μM TSA). After incubation for an additional 30 min at 30°C, the amount of free AMC was measured by monitoring the fluorescence intensity (EX = 380 nm, EM = 485 nm) using a Jobin Yvon FluoroMax-3 spectrofluorometer.

Results and discussion

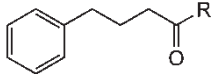
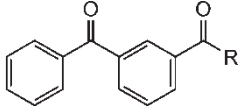
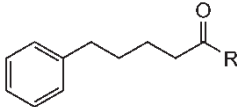
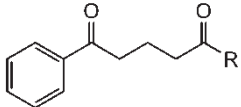
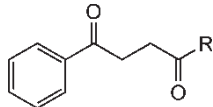
The fatty acids and the synthesized hydroxamate analogs were tested for their ability to inhibit the activity of rat-liver HDAC using a fluorescently labeled, acetylated, tripeptide mimic of the native acetylated lysine substrate. As 4-phenylbutyric acid and 5-phenylvaleric acid are reported to be millimolar-level inhibitors, all compounds were initially tested at 1 mM. The percent inhibition of these compounds is reported relative to the activity of HDAC in the presence of DMSO only (Table I). 4-Phenylbutyric acid and 5-phenylvaleric acid are consistent with the IC_{50} values of 0.64 mM and 1.4 mM previously reported [30]. The percent inhibition of TSA at 200 nM was also measured and found to be 70–85% under these conditions. Previous studies report the IC_{50} of TSA to be between 2–26 nM [11]. These small discrepancies can be explained due to differences in the assay method and enzyme source.

Comparison of the carboxylic acid compounds **1**, **5**, **9**, **13**, and **17** to the hydroxamic acids **2**, **6**, **10**, **14**, and **18** shows significant improvement in inhibition as would be expected by the bidentate binding of the hydroxamate to the Zn^{+2} cation versus the monodentate binding of the carboxylic acid. The greatest inhibition was seen with compounds **6** and **18**. The IC_{50} values were determined for **6** and **18** and were found to be 5 μM and 133 μM respectively (Figure 3). These values are in line with a previously determined IC_{50} value of 1.5 μM for 5-benzoylvaleric acid hydroxamate [31]. Although the values show **6** and **18** to be less effective than other hydroxamates such as TSA and SAHA, they show increased efficacy when compared to other derivatives of 4-phenylbutyric acid and valproic acid [18].

Analysis of the 4-phenylbutyric analogs and the 3-benzoylpropanoic analogs shows the additional carbonyl on chains of equal length to have a small negative effect on inhibition. This affect is less significant when comparing chains one carbon longer in length as seen by comparison of the 5-phenylvaleric analogs to the 3-benzoylbenzoic and 4-benzoylbutyric analogs. It was hoped that this would help inhibition as amide cap groups, such as that found in SAHA, have proven to be beneficial. Perhaps the shorter chain lengths in these compounds when compared to SAHA alter the placement of the carbonyl and negate the benefit provided by this group.

Crystallographic and modeling studies of TSA and SAHA in the catalytic core of HDAC predict that three key H-bonds are formed between the carbonyl oxygen, the NH and the OH to a tyrosine and two histidines respectively. The only methylated hydroxamate previously reported was an O-methyl, phenylamide derivative of TSA with a five carbon linker chain. It had an IC_{50} value greater than 10 μM [11]

Table I. Percent inhibition of short chain fatty acids and their hydroxamate analogs. All compounds were evaluated at 1 mM using rat liver HDAC.

Compound	Percent inhibition	Compound	Percent inhibition
4-phenylbutyric		3-benzoylbenzoic	
			
R = 1 = OH	13	R = 13 = OH	8
2 = NHOH	69	14 = NHOH	78
3 = NCH ₃ OH	42	15 = NCH ₃ OH	71
4 = NCH ₃ OCH ₃	64	16 = NCH ₃ OCH ₃	26
5-phenylvaleric		4-benzoylbutyric	
			
R = 5 = OH	37	R = 17 = OH	17
6 = NHOH	84	18 = NHOH	81
7 = NCH ₃ OH	39	19 = NCH ₃ OH	36
8 = NCH ₃ OCH ₃	24	20 = NCH ₃ OCH ₃	56
3-benzoylpropanoic			
			
R = 9 = OH	21		
10 = NHOH	45		
11 = NCH ₃ OH	8		
12 = NCH ₃ OCH ₃	36		

while the corresponding hydroxamate had an IC₅₀ value of 0.57 μM. Therefore, it was expected that we would see a drop in inhibition when the N-methylhydroxamate analogs (3, 7, 11, 15, and 19)

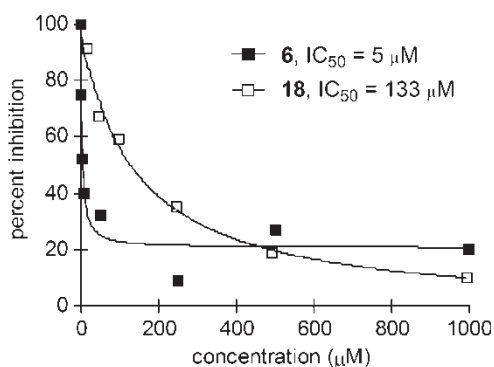


Figure 3. IC₅₀ determination of 5-phenylvaleric hydroxamic acid (6) and 4-benzoylbutyric hydroxamic acid (18).

were compared to the hydroxamates (2, 6, 10, 14, and 18) due to loss of one of these key H-bonds. For compounds 3, 15, and 19, the N-methyl hydroxamates still provided a benefit over the carboxylic acid binding groups. A surprising result was the increased inhibition of 4, 12, and 20 over their N-methyl counterparts despite the loss of a second H-bond. This could be explained by increased electron donating ability of the methoxy group relative to the hydroxy resulting in tighter binding to the Zn⁺² cation. It is unclear why compounds 8 and 16 do not show this trend. They are, however, on the extremes of conformational flexibility for this series of compounds and may have increased steric or hydrophobic constraints from the two methyl groups within the active site.

The body of data collected for TSA analogs has revealed that five to six carbons in the linking region to be an optimal length for inhibition [3,11]. Hydroxamate compounds that contained a benzoyl cap group also showed an increase in inhibition with increasing chain length where six intervening methylene groups were found to be optimal [31]. Previous studies of other phenyl substituted fatty acids from 4-phenylbutyric acid through 10-phenyldecanoic acid however did not show a clear trend of increasing inhibition with increasing chain length. Our results also show increased inhibition with increased linker regions for the hydroxamic acids but not for the carboxylic acids. As the substituted hydroxamates also do not show a clear trend in this regard, it appears that when the key hydrogen bonds afforded by the hydroxamate are absent, the exact placement of the Zn binding group in the active site is less critical.

This preliminary investigation of hydroxamic acid analogs of short-chain fatty acids shows the potential of combining characteristics of these two inhibitor types. Although relatively simple in structure, phenyl or benzoyl substituted fatty acids provide an economically and synthetically accessible platform for inhibitors. Modification of the carboxylate moiety to a hydroxamate provides increased inhibition while substitution with an N,O-dimethyl hydroxamate could provide effective inhibitors with longer residence times *in vivo*.

Acknowledgements

We gratefully acknowledge the McLaren Regional Medical Center and the University of Michigan-Flint Office of Research for funding this research.

References

- [1] Strahl BD, Allis CD. The language of covalent histone modifications. *Nature* 2000;403:41–45.

- [2] Grozinger CM, Schreiber SL. Deacetylase enzymes: biological functions and the use of small-molecule inhibitors. *Chem Biol* 2002;9:3–16.
- [3] Rodriguez M, Aquino M, Bruno I, De Martino G, Taddei M, Gomez-Paloma L. Chemistry and biology of chromatin remodeling agents: state of art and future perspectives of HDAC inhibitors. *Curr Med Chem* 2006;13:1119–1139.
- [4] Yoshida M, Hoshikawa Y, Koseki K, Mori K, Beppu T. Structural specificity for biological activity of trichostatin A, a specific inhibitor of mammalian cell cycle with potent differentiation-inducing activity in Friend leukemia cells. *J Antibiot* 1990;43:1101–1106.
- [5] Vigushin DM, Ali S, Pace PE, Mirsaidi N, Ito K, Adcock I, Coombes RC. Trichostatin A is a histone deacetylase inhibitor with potent antitumor activity against breast cancer in vivo. *Clin Cancer Res* 2001;7:971–976.
- [6] Monneret C. Histone deacetylase inhibitors. *Eur J Med Chem* 2005;40:1–13.
- [7] Sambucetti L, Fischer D, Zabludoff S, Kwon PO, Chamberlin H, Trogani N, Xu H, Cohen D. Histone deacetylase inhibition selectively alters the activity and expression of cell cycle proteins leading to specific chromatin acetylation and antiproliferative effects. *J Biol Chem* 1999;274:34940–34947.
- [8] Richon VM, Sandhoff TW, Rifkind RA, Marks PA. Histone deacetylase inhibitor selectively induces p21WAF1 expression and gene-associated histone acetylation. *Proc Natl Acad Sci USA* 2000;97:10014–10019.
- [9] Klisovic DD, Katz SE, Effron D, Klisovic MI, Wickham J, Parthun MR, Guimond M, Marcucci G. Depsipeptide (FR901228) inhibits proliferation and induces apoptosis in primary and metastatic human uveal melanoma cell lines. *Invest Ophthalmol Vis Sci* 2003;44:2390–2398.
- [10] Finnin MS, Donigian JR, Cohen A, Richon VM, Rifkind RA, Marks PA, Breslow R, Pavietich NP. Structures of a histone deacetylase homologue bound to the TSA and SAHA inhibitors. *Nature* 1999;401:188–193.
- [11] Xie A, Liao C, Li Z, Ning Z, Hu W, Lu X, Shi L, Zhou J. Quantitative structure-activity relationship study of histone deacetylase inhibitors. *Curr Med Chem-Anti-Cancer Agents* 2004;4:273–299.
- [12] Nielsen TK, Hildmann C, Dickmanns A, Schwienhorst A, Ficner R. Crystal structure of a bacterial class 2 histone deacetylase homologue. *J Mol Biol* 2005;354:107–120.
- [13] Santini V, Gozzini A, Scappini B, Grossi A, Ferrini PR. Searching for the magic bullet against cancer: the butyrate saga. *Leukemia Lymphoma* 2001;42:275–289.
- [14] Prasad KN. Butyric acid: A small fatty acid with diverse biological functions. *Life Sci* 1980;27:1351–1358.
- [15] Nguyen TD, Kim U-S, Perrine SP. Novel short chain fatty acids restore chloride secretion in cystic fibrosis. *Biochem Biophys Res Comm* 2006;342:245–252.
- [16] Phiel CJ, Zhang F, Huang EY, Guenther MG, Lazar MA, Klein PS. Histone deacetylase is a direct target of valproic acid, a potent anticonvulsant, mood stabilizer and teratogen. *J Biol Chem* 2001;276:36734–36741.
- [17] Suzuki T, Miyata N. Non-hydroxamate histone deacetylase inhibitors. *Curr Med Chem* 2005;12:2867–2880.
- [18] Gurvich N, Tsygankova OM, Meinkoth JL, Klein PS. Histone deacetylase is a target of valproic acid-mediated cellular differentiation. *Cancer Res* 2004;64:1079–1086.
- [19] Eyal S, Yagen B, Shimshoni J, Bialer M. Histone deacetylases inhibition and tumor cells cytotoxicity by CNS-active VPA constitutional isomers and derivatives. *Biochem Pharmacol* 2005;69:1501–1508.
- [20] Kuendgen A, Knipp S, Fox F, Strupp C, Hildebrandt B, Steidl C, Germing U, Haas R, Gattermann N. Results of a phase 2 study of valproic acid alone or in combination with all-trans retinoic acid in 75 patients with myelodysplastic syndrome and relapsed or refractory acute myeloid leukemia. *Ann Hematol* 2005;84:61–66.
- [21] Yoshida M, Kijima M, Akita M, Beppu T. Potent and specific inhibition of mammalian histone deacetylase both in vivo and in vitro by trichostatin A. *J Biol Chem* 1990;265:17174–17179.
- [22] Yoshida M, Kijima M, Akita M, Beppu T. Potent and specific inhibition of mammalian histone deacetylase both in vivo and in vitro by trichostatin A. *J Biol Chem* 1990;265:17174–17179.
- [23] Amato I. Pulling genes' strings. *C & EN* 2006;84(29):13–20.
- [24] Qiu L, Kelso MJ, Hansen C, West ML, Fairlie DP, Parsons PG. Anti-tumor activity in vitro and in vivo of selective differentiating agents containing hydroxamate. *Br J Cancer* 1999;80:1252–1258.
- [25] Nervi C, Borello U, Fazi F, Buffa V, Pelicci PG, Cossu G. Inhibition of histone deacetylase activity by trichostatin A modulates gene expression during mouse embryogenesis without apparent toxicity. *Cancer Res* 2001;61:1247–1249.
- [26] Whittaker M, Floyd CD, Brown P, Gearing AJH. Design and therapeutic application of matrix metalloproteinase inhibitors. *Chem Rev* 1999;99:2735–2776.
- [27] Mulder GJ, Meerman JHN. Sulfation and glucuronidation as competing pathways in the metabolism of hydroxamic acids: The role of N,O-sulfonation in chemical carcinogenesis of aromatic amines. *Envir Health Persp* 1983;49:27–32.
- [28] Sanderson L, Taylor GW, Aboagye EO, Alao JP, Latigo JR, Coombes RC, Vigushin DM. Plasma pharmacokinetics and metabolism of the histone deacetylase inhibitor trichostatin A after intraperitoneal administration to mice. *Drug Metab Dispos* 2004;32:1132–1138.
- [29] Wegener D, Wirsching F, Riester D, Schwienhorst A. A fluorogenic histone deacetylase assay well suited for high-throughput activity screening. *Chem Biol* 2003;10:61–68.
- [30] Lea MA, Shareef A, Sura M. Induction of histone acetylation and inhibition of growth by phenyl alkanolic acids and structurally related molecules. *Cancer Chemother Pharmacol* 2004;54:57–63.
- [31] Woo SH, Frechette S, Khalil EA, Bouchain G, Vaisburg A, Bernstein N, Moradei O, Leit S, Allan M, Fournel M, Trachy-Bourget M-C, Li Z, Besterman JM, Delorme D. Structurally simple trichostatin A-like straight chain hydroxamates as potent histone deacetylase inhibitors. *J Med Chem* 2002;45:2877–2885.

Copyright of *Journal of Enzyme Inhibition & Medicinal Chemistry* is the property of Taylor & Francis Ltd and its content may not be copied or emailed to multiple sites or posted to a listserv without the copyright holder's express written permission. However, users may print, download, or email articles for individual use.